View Online / Journal Homepage
Dynamic Article Links

Lab on a Chip

Cite this: DOI: 10.1039/c2lc40546f

www.rsc.org/loc

PAPER

Drop formation in non-planar microfluidic devices†

Assaf Rotem,*[a] Adam R. Abate,[b] Andrew S. Utada,[c] Volkert Van Steijn[d] and David A. Weitz[e]

Received 11th May 2012, Accepted 28th June 2012
DOI: 10.1039/c2lc40546f

Microfluidic devices can be used to produce single or multiple emulsions with remarkably precise control of both the contents and size of the drops. Since each level of a multiple emulsion is formed by a distinct fluid stream, very efficient encapsulation of materials can be achieved. To obtain high throughput, these devices can be fabricated lithographically, allowing many devices to operate in parallel. However, to form multiple emulsions using a planar microfluidic device, the wettability of its surface must switch from hydrophobic to hydrophilic on the scale of micrometers where the drops are formed; this makes the fabrication of the devices very difficult. To overcome this constraint, we introduce non-planar microfluidic devices with graduated thicknesses; these can make drops even when their wetting properties do not favor drop formation. Nevertheless, the dependence of drop formation on the device geometry, the flow rates and the properties of the fluids, particularly in the case of unfavorable wetting, is very complex, making the successful design of these devices more difficult. Here we show that there exists a critical value of flow of the continuous phase above which drop formation occurs; this value decreases by two orders of magnitude as the wetting to the device wall of the continuous phase improves. We demonstrate how this new understanding can be used to optimize device design for efficient production of double or multiple emulsions.

Introduction

Multiple emulsions, or drops within drops, are of great importance technologically for encapsulating chemicals, reagents or drugs in more robust structures; for example, a single drop within a larger drop, forming a core–shell structure, can provide an important means of encapsulation and release of materials.[1–7] Control over the size of the innermost drop provides a means to adjust the amount of encapsulated material, whereas control over the thickness of the shell provides a means to adjust the nature of the encapsulation. Double emulsions can be formed with microfluidic devices, which provide precise control over the size and shape of the drops. Such microfluidic devices can be easily fabricated using capillary tubes, which enable the facile formation of multiple emulsions.[8] However, since each device is custom made, it is very difficult to produce them in the high numbers necessary to create large quantities of multiple emulsions required for practical uses. In contrast, microfluidic devices formed by stamping or lithographic techniques provide a route to scale up the method for the production of large quantities of multiple emulsions.[9] With these devices however, the wettability of the surfaces must be precisely controlled to make drops; as opposed to most capillary-based microfluidic devices, where the dispersed phase orifice is much smaller than the collection channel surrounding it, the orifice in lithographically-produced channels is usually as deep as its collection channels, and thus, when the continuous phase meets the dispersed phase to form drops, the latter is no longer geometrically engulfed by the continuous phase as is the case with capillary devices. Instead, drop formation can only occur if the wettability of the surface strongly favors the continuous phase, enabling it to wet the surface instead of the dispersed phase, thereby separating the dispersed phase from the device surface to form a drop. For example, to form drops of water in oil, the channels must be hydrophobic, so that the water will have a tendency to de-wet from the channel walls and become dispersed in the oil. In contrast, to form drops of oil in water the channels must be hydrophilic. The necessity for such control is exacerbated when double emulsions are formed, because the wettability of the walls must change between the first and the second drop-making junctions, just tens of microns apart.[10–12]

To overcome these stringent requirements for the control of wettability, non-planar microfluidic devices can be fabricated such that the orifice has a smaller cross sectional area than the collection channel, enabling the continuous phase to flow fully around the dispersed phase.[13,14] In this case, the continuous

[a]*Department of Physics and School of Engineering and Applied Sciences, Harvard University, 11 Oxford St., Cambridge, MA 02138, United States. E-mail: arotem@seas.harvard.edu*
[b]*Department of Bioengineering and Therapeutic Sciences, California Institute for Quantitative Biosciences, University of California, San Francisco, 505 Parnassus Avenue, San Francisco, CA 94122, United States*
[c]*Bioengineering Department, University of California, Los Angeles, 405 Hilgard Avenue, Los Angeles, CA 90095, United States*
[d]*Delft University of Technology, Department of Chemical Engineering, Julianlaan 136, 2628 BL Delft, the Netherlands*
[e]*Department of Physics and School of Engineering and Applied Sciences, Harvard University, 29 Oxford St., Cambridge, MA 02138, United States*
† Electronic Supplementary Information (ESI) available. See DOI: 10.1039/c2lc40546f

phase fully surrounds the dispersed phase, helping to de-wet it from the walls, and drops are formed even when the wettability of the channels favors the dispersed phase. This significantly simplifies device fabrication. However, tuning the operation of a non-planar microfluidic drop maker remains a delicate process, which is sensitive to the geometry of the device, the properties of the fluids and the wettability of the surface. The design of such non-planar devices requires knowledge of the key parameters[15–17] that affect their performance, particularly when the wetting conditions are not favorable.

In this paper we describe a simple method to fabricate non-planar devices that make drops under unfavorable surface wetting conditions, in which a planar device would not work. We show that the flow rate of the continuous phase must exceed a critical value for drop formation; moreover, this critical value strongly depends on the contact angle of the triple line connecting the two fluid phases and the device wall. We provide guidelines for the operation of these non-planar microfluidic devices, enabling the production of double emulsions.

Results

The basic drop making geometry used in our experiments consists of a central inlet channel, of depth h_s and width w_s, which introduces the dispersed phase into the junction, and two side channels, of depth h and width L, which introduce the continuous phase. The two phases are collected through an outlet channel, of depth h and width w, as illustrated in Fig. 1a. We focus on non-planar junctions, where $h_s < h$, and where we center the inlet channel both horizontally and vertically with respect to the outlet channel. During drop formation, the dispersed phase forms a spherical cap that is centered on the orifice of the central inlet channel. The base of the cap has a radius r, and the angle of the cap, θ, is the triple-line contact angle,[18] as illustrated in Fig. 1b. The total flow rate of the continuous phase is q, and the flow rate of the dispersed phase is maintained well below q. For comparison we also investigate planar junctions where $h_s = h$.

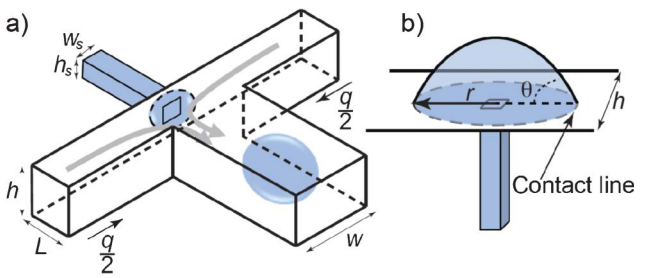

Fig. 1 Geometry of the non-planar junction. a) The dispersed phase (blue) flows into a junction of height h through a central inlet of width w_s and height h_s, which is centered vertically with respect to the outlet nozzle. The continuous phase (black arrows) flows at a total rate q through two side channels of width L and height h. The interface between the fluids forms a spherical cap and both fluids are collected *via* an outlet channel of width w and height h. b) A different view shows the triple contact line (dashed line), where the two phases and the device meet. The triple line lies on the circumference of the base of the spherical cap and has a radius r. The triple line contact angle, θ, is measured between the two phases and the vertical wall on a plane that is perpendicular to the triple line.

Planar devices

To investigate the role of wetting in drop formation we study planar devices, and use several different combinations of fluids, different device materials and different wall coatings; in each case we characterize the device by the contact angle and determine whether drops are formed. We find a sharp change in behavior when $\theta = 90°$. When the continuous phase preferentially wets the walls ($\theta > 90°$), planar devices form drops even at minimum flow rates of the continuous phase ($q_{min} = 50\ \mu L\ h^{-1}$). In contrast, when the dispersed phase preferentially wets the walls ($\theta < 90°$), the planar devices do not form drops even at the maximum possible flow rate of the continuous phase ($q_{max} = 50\ mL\ h^{-1}$), which is limited by the bond strength of the device. Thus, in planar devices, drop formation is strongly dependent on the wetting conditions and is only feasible in the favorable case when the continuous phase wets the walls of the device more strongly. All of the results for planar devices are summarized in Table 1.

Non-planar devices

Non-planar devices remove the constraints on wettability imposed by the planar geometry; drops can be formed even in unfavorable wetting conditions. To demonstrate this, we emulsify water containing 50% (w/w) glycerol in a fluorocarbonated oil (HFE 7500) using a non-planar PDMS drop maker coated with parylene. Even though the water phase wets the coated channels better than the oil phase, with a measured static contact angle of $\theta = 60°$, the device forms drops of water in oil. As the dispersed phase first flows into a non-planar junction it partially wets the walls adjacent to the central inlet and forms a spherical cap with a fixed dynamic contact angle, as shown in Fig. 2. As the cap grows, the shear exerted by the continuous phase on its interface also grows; ultimately, this shear is large enough to prevent further growth of the cap and to instead cause periodic drop formation. If q is then decreased, the cap again grows and eventually touches the top and bottom of the main channel, enabling the dispersed phase to wet the wall, and drops are no longer formed as shown in Fig. 3a.

To quantify this behavior, we identify the critical flow rate of the continuous phase, q_c, that separates drop formation from the flow of the dispersed phase along the device walls. We determine the value of q_c by decreasing the flow rate and calculating the average between the smallest value of q that still produces drops and the largest that does not. We find that q_c is strongly hysteretic; its value is nearly 10 times higher for increasing q than it is for decreasing q. Moreover, the value of q_c varies for subsequent measurements. These observations are consistent with there being a strong history dependence on the wetting conditions of the surface. Thus we restrict our measurements to those performed in unused devices and made with decreasing q. In addition, we find that the flow rate of the dispersed phase has a negligible effect on q_c, provided its value is well below that of the continuous phase; when the flow rates become comparable there is a significant dependence of q_c on the flow rate of the dispersed phase. Thus, wherever possible, we restrict our

Table 1 Operation of planar devices: drop making results for a variety of device materials, coatings and fluids. In all cases where $\theta < 90°$, q_c was larger than the maximum available flow rate and drops could not be formed; in all cases where $\theta > 90°$, q_c was smaller than the minimum available flow rate and the device formed drops continuously. Abbreviations: PVA—polyvinyl alcohol, MW 13 000–23 000 g mol^{-1}, 87–89% hydrolyzed, Sigma; DC—Dow Corning Fluid; HFE—HFE-7500 fluorocarbon oil, 3 M; PDMS—polydimethylsiloxane; Apex Glass—see Methods; ODS—methyl-octadecyl-dichlorosilane coating; O_2 plasma—device under the effects of plasma treatment, see Methods; Aquapel—device coated with Aquapel, see Methods

Dispersed phase	Continuous phase	Device	θ (°)	drops?
Water	36% (w/w) chloroform in hexane	Apex Glass	16 ± 1	no
Water	1.8% (w/w) R22 in HFE	PDMS	45 ± 5	no
Water	DC 200 0.65cSt	O_2-treated PDMS	60 ± 5	no
Water	DC 200 5cSt	O_2-treated PDMS	60 ± 5	no
Water	DC 510 50cSt	O_2-treated PDMS	60 ± 5	no
HFE	Water	PDMS	62 ± 3	no
HFE	Water	O_2-treated PDMS	81 ± 3	no
Water	HFE	O_2-treated PDMS	99 ± 3	yes
Water	HFE	PDMS	117 ± 3	yes
3% (w/w) PVA in water	2% (w/w) EM90 in 1-octanol	Aquapel-treated PDMS	133 ± 3	yes
3% (w/w) PVA in water	2% (w/w) EM90 in 1-octanol	PDMS	150 ± 3	yes
3% (w/w) PVA in water	1.8% (w/w) R22 in HFE	O_2-treated PDMS	150 ± 5	yes
3% (w/w) PVA in water	1.8% (w/w) R22 in HFE	PDMS	150 ± 5	yes
Water	1.8% (w/w) R22 in HFE	O_2-treated PDMS	154 ± 2	yes
Water	36% (w/w) chloroform in hexane	ODS-treated Apex Glass	165 ± 2	yes

measurements to values of the dispersed phase flow rate less than one tenth of that of the continuous phase.

To test the dependence of q_c on both the wetting properties of the fluids and the device geometry, we plot the mean critical velocity of the continuous phase in the side channel, $U_c = q_c/2hL$, as a function of the device dimensions and of θ. While there is no apparent dependence of U_c on L, h or Lh, as shown in Fig. 4a–c, it does exhibit a marked dependence on θ, decreasing dramatically for contact angles approaching 90° as shown in Fig. 4d. To quantify this dependence, we calculate the critical capillary number, $Ca_c = \mu U_c/\gamma$, where μ is the viscosity of the continuous phase and γ is the interfacial tension between the continuous and dispersed phases. We plot Ca_c as a function of θ. As in planar devices, drops form at any Ca value when the continuous phase preferentially wets the walls ($\theta > 90°$). However, in non-planar devices, drops can also form when the dispersed phase preferentially wets the walls ($\theta < 90°$) for $Ca > Ca_c$, as shown in Fig. 5.

Remarkably, Ca_c decreases monotonically by two orders of magnitude as θ approaches 90°. This trend can be explained using geometrical considerations: for θ close to 90°, most of the cross-section of the side channels, hL, available for continuous flow is excluded by the spherical cap, which nearly plugs the channel.[19,20]

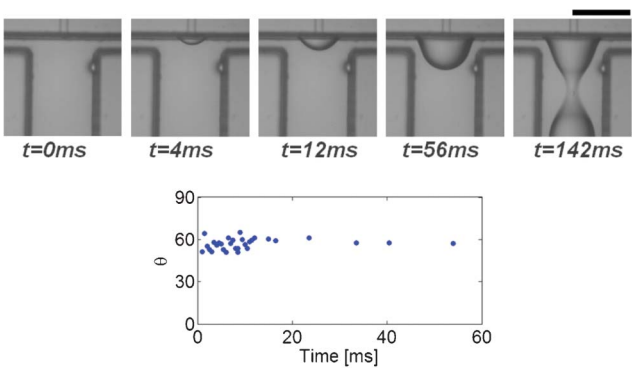

Fig. 2 Top: Time sequence of the formation of aqueous (50% (w/w) glycerol in water) drops in oil (HFE 7500) in a non-planar PDMS channel coated with parylene. Water flows from the small channel into the junction at a rate of 0.1 mL h^{-1}, where it partially wets the adjacent walls, forming a cap (t = 0 ms, t = 12 ms). This cap continues to grow with a fixed $\theta \sim 60°$ until the shear applied by the continuous phase, supplied at a rate of q = 15 mL h^{-1} from the side channels, deforms the cap (t = 56 ms) resulting in the release of a droplet (t = 142 ms). Scale bar: 200 μm. See also supplementary movie 1.† Bottom: θ measured from the top movie plotted as a function of time lapsed from first appearance of the forming drop.

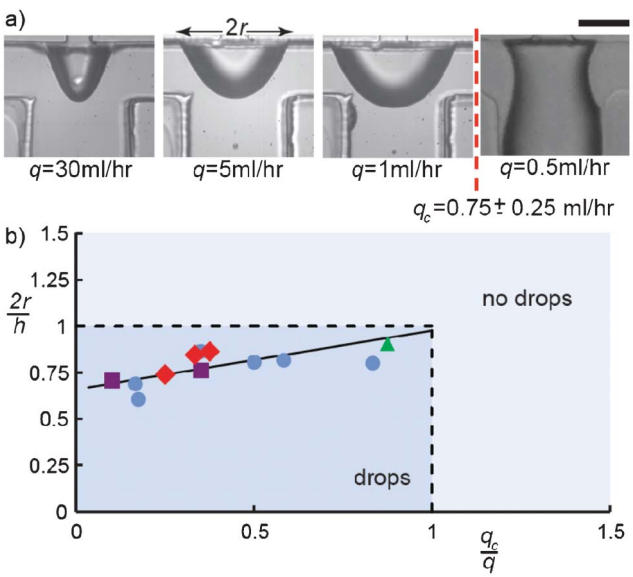

Fig. 3 Formation of aqueous (50% (w/w) glycerol in water) drops in oil (HFE 7500) in PDMS channels coated with parylene for decreasing rates of flow, q, of the continuous phase (left to right). For q below q_c = 0.75 ± 0.25 mL h^{-1}, drops are no longer released from the cap and the aqueous phase wets the walls of the main channel (right). Scale bar: 50 μm. See also supplementary movie 2.† b) The radius of the spherical cap base normalized by the height of the device is plotted against the inverse of the flow rate of the continuous fluid normalized by q_c. The radius increases with decreasing flow rate and reaches a value of unity for $q = q_c$. For $q_c/q > 1$, drops no longer form as the dispersed phase wets the walls of the main channel. Geometry: (w_s, h_s, w, h) = (25, 25, 125, 125) μm and L = 10 μm (circles), L = 20 μm (squares), L = 40 μm (triangles), L = 62.5 μm (diamonds). Static contact angle $\theta \sim 60°$.

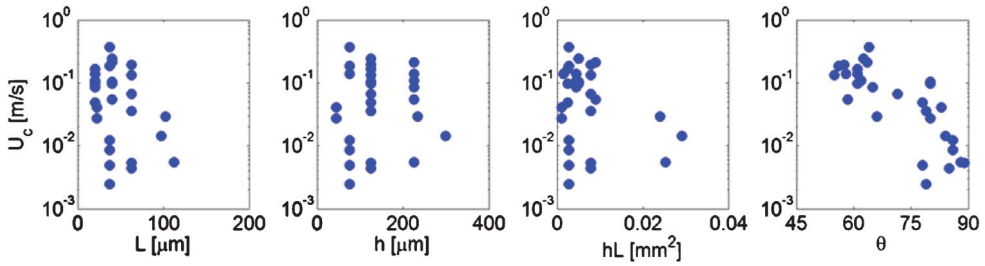

Fig. 4 Critical flow velocity U_c required to reproducibly form drops as a function of the geometry of the device and of θ.

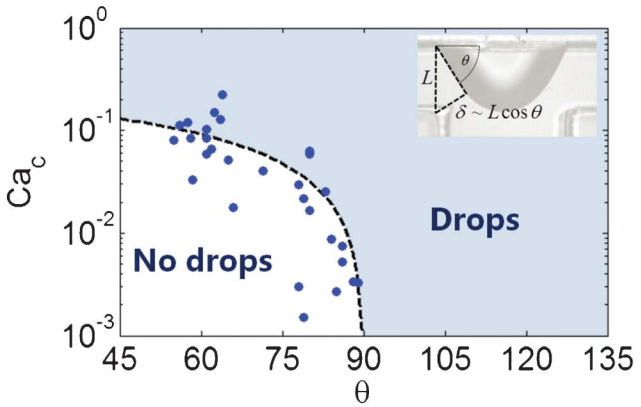

Fig. 5 The critical capillary number as a function of the dynamic contact angle as measured for drop makers with varying geometry. For $\theta < 90°$, drops are formed only when the capillary number is higher than the critical value Ca_c. For $\theta > 90°$, the continuous phase preferentially wets the walls and drops are formed regardless of the capillary number. Dashed line is a fit of the Cosine function to the data. Inset: approximating the cross-sectional gap δ between the side channel and the forming drop. For $L < h$, δ can be approximated as $L\cos\theta$.

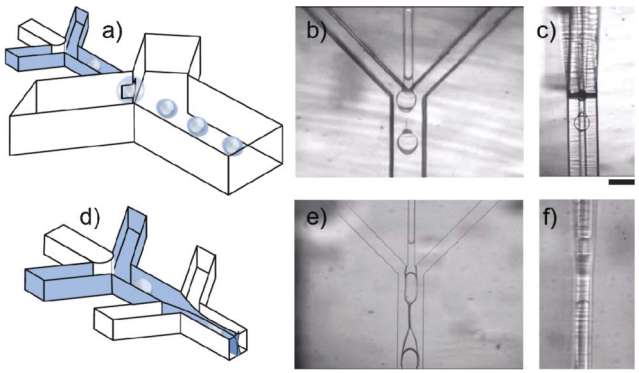

Fig. 6 Non-planar devices for making double emulsions. a) A schematic drawing of a hydrophobic non-planar device with water drops (white) forming at the planar first junction, and oil drops (blue) wrapping the water drops at the second, non-planar junction. b) Top view of a real non-planar junction, similar to the second junction in the schematics, as it is making drops. See also supplementary movie 3.† c) Side view of the same junction in (b). See also supplementary movie 4.† d) A schematic drawing of a hydrophobic planar device with water drops forming at the first junction and a sheath of oil that wets the floor and ceiling wrapping the water drops at the second junction. e) Top view of a real planar junction similar to the second junction in the schematics, as it is making drops. See also supplementary movie 5.† f) Side view of the same junction in (e). See also supplementary movie 6.† Scale bar is 100 μm.

Consequently, the flow velocity of the continuous phase and the shear force it applies on the cap increases. For the device geometries used in our experiment, the minimum cross-sectional gap δ can be approximated by $L\cos\theta$, as shown in the inset of Fig. 5.

Although the capillary number dominates the detailed mechanism of drop formation in unconfined systems,[8] its selection as the dimensionless parameter in our experiments remains to be justified with further experiments. Nevertheless, we have shown that, in confined systems, drop formation depends strongly on the contact angle between the fluid phases and the device. In the case of planar devices this dependence is a step function,

$$Ca_c \sim \Theta(90^\circ - \theta)$$

where Θ is the step function, while in the non-planar devices used here we suggest that this dependence can be approximated by

$$Ca_c \sim \cos\theta \cdot \Theta(90^\circ - \theta)$$

Double emulsion drops in non-planar devices

An important application of the non-planar drop maker is the production of double emulsions, without the need to locally modify the wettability of the channel walls. We demonstrate this by producing water/oil/water double emulsions in the hydrophobic channel network shown in Fig. 6a. The hydrophobic walls are favorable for making water drops in oil, and hence a planar junction is used for the inner drops. To produce double emulsions, these drops and the surrounding oil are subsequently emulsified at the second junction, which requires a non-planar geometry to facilitate drop formation. The shear exerted on the cap forming in the second junction is sufficiently large to prevent the middle oil phase from wetting the walls of the main channel, as is evident from the top-view image in Fig. 6b and the side-view image in Fig. 6c. By contrast, when using a planar geometry in the second junction (Fig. 6d), the middle oil phase wets the walls even at high flow rates of the continuous water phase, and the formation of double emulsions is not possible; instead, the middle phase co-flows with the continuous phase along the device walls, as shown in Fig. 6e and Fig. 6f. The design can be modified to produce oil/water/oil double emulsions by using a non-planar geometry for the first junction, or to make multiple emulsions by using sequential drop-making junctions.

Although the formation of double emulsions in non-planar drop makers should be possible for a wide range of fluids and wall properties, some combinations require impractically large flow rates of the continuous phase to prevent the dispersed phase from wetting the walls. These are ultimately limited by the bond strength of the device. Increasing θ towards 90° can reduce these flow rates substantially, as shown in Fig. 5; however, θ cannot be increased above 90° or the inner drops cannot be produced in the planar junction upstream. Tuning θ can be achieved by coating the device with functional layers.[21,22] The critical flow rate may be further decreased by using side channels of smaller cross-sectional area hL, and by using angled junctions.[9]

Summary & outlook

In planar devices, drops form only if the continuous phase preferentially wets the walls; by contrast, when using non-planar devices drops can also form when the dispersed phase preferentially wets the walls, given that the flow rate of the continuous phase is sufficiently large to prevent the dispersed phase from wetting the channel walls. The minimum required flow rate of the continuous phase to operate these devices decreases dramatically as the contact angle approaches 90°. These findings can be used as guidelines to design non-planar drop makers to ensure the minimally required flow rate does not exceed practical limitations. We demonstrate the formation of double emulsion drops in non-planar devices, and we expect that those devices can also be used to make emulsions of higher order complexity.

Methods and materials

Fabrication of devices

We make planar devices using two different materials: polydimethylsiloxane (PDMS) and Apex glass. We make PDMS devices using replica molding with SU8 photo resist as the mold master,[23] and the Apex Glass devices are custom made by Life BioScience Inc. (Albuquerque, NM, USA). We make non-planar devices from PDMS; since it is topologically impossible to make non-planar junctions using a single photolithographic mold, we first make two complementary molds, one for the top part of the non-planar junction and a second for the bottom part. Each of the molds consists of two layers, as shown in Fig. 7a. The multilayered molds are fabricated *via* a two-step UV exposure, applying a second photo-resist layer between the two exposures and aligning the second exposure with the first using a mask aligner (ABM, CA). After replicating the top and bottom molds with PDMS, we align the two replicas using a "mortise and tenon" method[24,25] by matching positive features on one side with negative features on the other, as shown in Fig. 7b. After treating both sides with oxygen plasma, we apply a drop of water for lubrication, match the two parts and bake dry at 65 °C for one hour to bond.

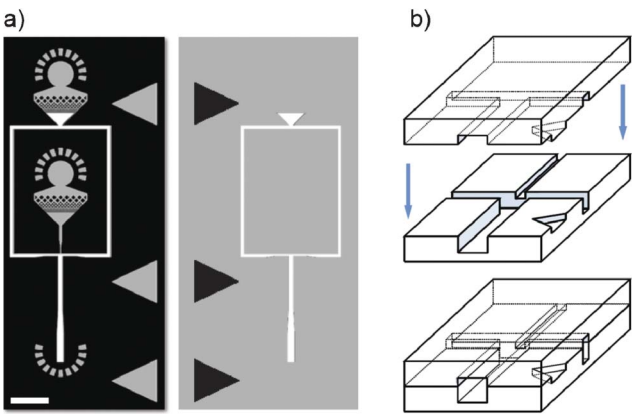

Fig. 7 Fabricating non-planar devices. a) Two photolithographic masters that are used for making the device. Each master has two layers: the base of the master is black, the first layer is gray and the second layer is white. Scale bar is 1 mm. b) Two PDMS molds, the top one replicated from the right master in (a) and the bottom one replicated from the left master in (a) are bonded face to face, with the triangles on both sides matching to align the molds and make the final device.

Wettability control of the devices

To control the contact angles in our devices we coat the channels or treat them with oxygen plasma. We render PDMS devices more hydrophilic by treating them with oxygen plasma and using them promptly, since the device wettability relaxes to the hydrophobic native state after several weeks at room temperature, or after several days at 65 °C. We render the PDMS devices more hydrophobic by coating them with Aquapel (Rider, MA, USA). We inject Aquapel into the devices and then dry the devices by blowing air into them and baking at 65 °C for 15 min. To flow organic solutions that would otherwise swell PDMS, we coated some PDMS channels with parylene.[22] We render the glass devices more hydrophobic by coating them with 5% methyl-octadecyl-dichlorosilane and 5% ethyl acetate in toluene. We inject the silane coating into the devices, wash the devices with clean hexane, and dry them by blowing air into them and baking at 65 °C for 15 min.

Measuring interfacial tension forces and contact angles

The interfacial tension was measured using Dunoy's ring method on a Sigma 700 tensiometer (Attension, Finland). The static contact angles were measured based on the static sessile drop method using a home-built goniometer. We also measured the dynamic contact angle during the formation of droplets in the microfluidic device by analyzing the drop shape from images. The static contact angles agree with the dynamic contact angles to within 15%.

Acknowledgements

This work was supported by the NSF (DMR-1006546) and the Harvard MRSEC (DMR-0820484). The authors also thank Capsum for financial support, Mark Romanowsky for experimental support and Shmuel Rubinstein for helpful discussions.

References

1 E. Lorenceau, Generation of polymerosomes from double-emulsions, *Langmuir*, 2005, **21**, 9183–9186.
2 B. J. Sun, H. C. Shum, C. Holtze and D. A. Weitz, Microfluidic melt emulsification for encapsulation and release of actives, *ACS Appl. Mater. Interfaces*, 2010, **2**, 3411–3416.

3 H. C. Shum, J. W. Kim and D. A. Weitz, Microfluidic fabrication of monodisperse biocompatible and biodegradable polymersomes with controlled permeability, *J. Am. Chem. Soc.*, 2008, **130**, 9543–9549.
4 C. H. Chen, R. K. Shah, A. R. Abate and D. A. Weitz, Janus particles templated from double emulsion droplets generated using microfluidics, *Langmuir*, 2009, **25**, 4320–4323.
5 M. H. Lee, S. G. Oh, S. K. Moon and S. Y. Bae, Preparation of Silica Particles Encapsulating Retinol Using O/W/O Multiple Emulsions, *J. Colloid Interface Sci.*, 2001, **240**, 83–89.
6 F. Cui, Preparation and characterization of melittin-loaded poly(DL-lactic acid) or poly(DL-lactic-*co*-glycolic acid) microspheres made by the double emulsion method, *J. Controlled Release*, 2005, **107**, 310–319.
7 A. R. Abate, Synthesis of monodisperse microparticles from non-newtonian polymer solutions with microfluidic devices, *Adv. Mater.*, 2011, **23**, 1757–1760.
8 A. S. Utada, Monodisperse double emulsions generated from a microcapillary device, *Science*, 2005, **308**, 537–541.
9 M. B. Romanowsky, A. R. Abate, A. Rotem, C. Holtze and D. A. Weitz, High throughput production of single core double emulsions in a parallelized microfluidic device, *Lab Chip*, 2012, **12**, 802–807.
10 A. R. Abate, J. Thiele, M. Weinhart and D. A. Weitz, Patterning microfluidic device wettability using flow confinement, *Lab Chip*, 2010, **10**, 1774–1776.
11 A. R. Abate, Photoreactive coating for high-contrast spatial patterning of microfluidic device wettability, *Lab Chip*, 2008, **8**, 2157–2160.
12 M. B. Romanowsky, Functional patterning of PDMS microfluidic devices using integrated chemo-masks, *Lab Chip*, 2010, **10**, 1521–1524.
13 F.-C. Chang and Y.-C. Su, Controlled double emulsification utilizing 3D PDMS microchannels, *J. Micromech. Microeng.*, 2008, **18**, 065018.
14 S. P. C. Sim, The shape of a step structure as a design aspect to control droplet generation in microfluidics, *J. Micromech. Microeng.*, 2010, **20**, 035010.
15 M. De Menech, P. Garstecki, F. Jousse and H. A. Stone, Transition from squeezing to dripping in a microfluidic T-shaped junction, *J. Fluid Mech.*, 2008, **595**, 141–161.
16 G. F. Christopher, N. N. Noharuddin, J. A. Taylor and S. L. Anna, Experimental observations of the squeezing-to-dripping transition in T-shaped microfluidic junctions, *Phys. Rev. E: Stat., Nonlinear, Soft Matter Phys.*, 2008, **78**, 036317.
17 P. Garstecki, M. J. Fuerstman, H. A. Stone and G. M. Whitesides, Formation of droplets and bubbles in a microfluidic T-junction-scaling and mechanism of break-up, *Lab Chip*, 2006, **6**, 437–446.
18 P.-G. De Gennes, F. Brochard-Wyart and D. Quéré, *Capillarity and wetting phenomena: drops, bubbles, pearls, waves*, Springer, 2004, p. 15.
19 A. R. Abate, A. Rotem, J. Thiele and D. A. Weitz, Efficient encapsulation with plug-triggered drop formation, *Physical Review E*, 2011, **84**, 031502.
20 D. Funfschilling, H. Debas, H. Z. Li and T. G. Mason, Flow-field dynamics during droplet formation by dripping in hydrodynamic-focusing microfluidics, *Phys. Rev. E: Stat., Nonlinear, Soft Matter Phys.*, 2009, **80**, 015301.
21 J. Thiele, *et al.*, Fabrication of polymersomes using double-emulsion templates in glass-coated stamped microfluidic devices, *Small*, 2010, **6**, 1723–1727, DOI: 10.1002/smll.201000798.
22 A. S. Utada, A. Rotem, A. R. Abate, D. Takeuchi and D. A. Weitz, Controlling chemical resistance and wettability of microfluidic devices using Chemical Vapor Deposition of parylene, 2011, in preparation.
23 J. C. McDonald, *et al.*, Fabrication of microfluidic systems in poly (dimethylsiloxane), *Electrophoresis*, **21**, 27–40.
24 H. Wu, T. W. Odom, D. T. Chiu and G. M. Whitesides, Fabrication of complex three-dimensional microchannel systems in PDMS, *J. Am. Chem. Soc.*, 2003, **125**, 554–559.
25 J. R. Anderson, *et al.*, Fabrication of topologically complex three-dimensional microfluidic systems in PDMS by rapid prototyping, *Anal. Chem.*, 2000, **72**, 3158–3164.